JOURNAL OF OPTOELECTRONICS AND ADVANCED MATERIALS Vol. 12, No. 3, March 2010, p. 686 - 691

Layout for millimeter wave Composite Right/Left Handed devices obtained by femtosecond laser ablation

M. ZAMFIRESCU*, G. SAJIN[a], A. BUNEA[a], F. CRACIUNOIU[a], S. SIMION[a], R. DABU
NILPRP – Bucharest, Atomistilor 409, 077125 Magurele, Romania
[a]IMT Bucharest, Str. Erou Iancu Nicolae 126A, 077190 Bucharest, Romania

In this paper, design and fabrication of Composite Right/Left-Handed (CRLH) structures for metamaterial based millimeter wave (MMW) devices and circuits are presented. Coplanar waveguide transmission lines working at tens of GHz, were obtained by laser ablation of thin gold films deposied on silicon. The samples are precisely processed by tightly focusing a femtosecond laser beam with 200 fs pulse duration, 775 nm wavelength, energy of hundreds of nJ per pulse, and repetition rate of 2 kHz. A 2D structure is generated by translating the sample according to a computed design. The lateral dimension of the lines removed by the laser from the evaporated film is controlled by adjusting the laser intensity and the focus position. Using this technique, the fabrication of micro-structures for millimeter wave devices is demonstrated.

(Received June 20, 2009; accepted November 16, 2009)

Keywords: Laser ablation, Millimeter wave, CRLH circuits

1. Introduction

The lasers start to be integrated in almost all stages of micro- and nanotechnologies from the fabrication of micro/nanoscale devices, to the characterisation, and even manipulation of small particles and cells [1-5]. The fabrication of micro-devices using lasers is possible by means of controlled modification of the materials under light irradiation. When an ultrafast laser beam with pico- or femtosecond pulse duration is tightly focalised on the surface of a solid sample, if the laser fluence exceeds a certain threshold, a small volume of material is ablated leaving behind patterns with micrometer or sub-micrometer dimensions [6-10]. Due to the long heat-diffusion time of almost all of materials compared to the pulse duration of commercially available femtosecond laser systems, the adjacent surface of the processed area remains almost unaffected. This characteristic makes the laser ablation with ultrafast lasers to become a processing technique suitable for configuration of microstructures on metallic films with application on microeletronics circuits, microsensors, or other MEMS.

Metallic or dielectric structures with resolution down to a few micrometres are traditionally done by photolithography which involves few protocol steps such as UV sensitive photoresist deposition, UV exposure, photoresist hardening, chemical layers corrosion. In contrast, the laser ablation technique is a direct writing method which allows the fabrication of a desired geometry in one step. Moreover, the laser ablation has the advantage to be easily employed in the processing on hard materials such as glass or ceramic, chemical inert materials like platinum and gold, or for any other material when an appropriate solution can't be found due to the chemical attack of the mask material while layer corrosion takes place. Its main drawback is related to the fact that being a scanning technique, the laser ablation is a time consuming method and its performances are limited by the precision and speed of the scanning mechanics. The laser processing of the materials suppose the focalization of the laser beam at the material surface using a focusing lens with high numerical aperture in order to obtain by laser evaporation very small structures with size of few micrometers or submicrometers. Dimensions even below 100 nm can be reached when the micro and nanoparticles are used as focussing optics, such as in the case of near-field laser processing [11-12]. In some particular designs the lateral dimension of the ablated spot has to be well controlled from the diffraction limit up to tens of micrometres.

In this work, the photolithography and laser ablation are both used for configuration of the metallic layers microstructures on large area, combining the advantages of each of the two techniques. Series of ablation measurements were produced on metallic films in order to establish the optimal parameter of the ablation. We controlled the size of the ablated area trough the laser energy and the focusing conditions. Composite Right/Left-Handed transmission lines (CRLH-TL) structures for millimeter waves exhibiting low loss and broad bandwidth were designed and produced by this method.

In the microwave frequency domain the CRLH-TLs are usually made in microstrip or CPW configuration and consist in series of interdigital capacitors and shunt stub inductances, with typical size of few millimeters and hundreds of micrometers of the interdigital width [13-15]. Such structures exhibit a negative phase velocity. When moving toward the frequency range of tens to hundreds of GHz, a considerable dimensions reduction of physical size of the unit cell is required. In this respect interdigital capacitors with fingers width of few micrometers have to

be considered [16]. At these dimensions, the classical photolitography reaches its limits and a new technological approach is necessary. The CPW (CoPlanar Waveguide) configuration is preferred in the millimeter wave domain because this approach allows the on-wafer characterization of the MIC and MMIC devices and circuits.

Part of the surface of the structures requiring resolution down to 10 μm and large processed area were realised by classical photolithography. Afterward, the small details of the structures were obtained by laser ablation with resolution down to 1 μm. Thin films of gold deposited on silicon were laser processed in order to create periodic structures. The conditions of the laser ablation of the metallic film are studied and the writing parameters of the structures are optimised.

2. CRLH structure for millimeter wave frequency band

2.1. CRLH structure for millimeter wave domain

The layout of a CRLH cell structure in CPW configuration for the millimeter wave frequency band is shown in the figure 1a. The cell structure is formed by two series connected interdigitated capacitors and a parallel inductance made as a CPW line to the ground. This structure may be processed on any kind of substrate, glass, or silicon. In this approach we choose a wafer of high resistivity silicon (5 kΩcm), in order to facilitate the fabrication of components compatible with MMIC (Monolithic Microwave Integrated Circuits) technology. The substrate used was silicon of high resistivity covered by thermal SiO_2 of 1μm thickness. Then, 20 nm Cr layer followed by 0.1μm Au has been evaporated on the entire surface.

The equivalent circuit of the studied CRLH structure is shown in figure 1b. Here, $2C_{Cs}$, $L_{Cs}/2$ and $2C_{Cp}$ are respectively capacity, inductance and equivalent capacity of the interdigitated capacitor and L_{Lp} and C_{Lp} are the inductance and respectively equivalent capacity of the CPW ground shorted stub inductor.

The design of our CRLH structure was done in such way that series resonance frequency (given by C_{Cs} and L_{Cs}) is equal with shunt resonance frequency (given by L_{Lp}, C_{Lp} and C_{Cp}), obtaining a balanced structure. Such a balanced CRLH structure may be used to obtain a series of millimeter wave devices: directional couplers, filters, leaky waves antennas and other, all having the advantage of reduced size comparing with classical similar devices.

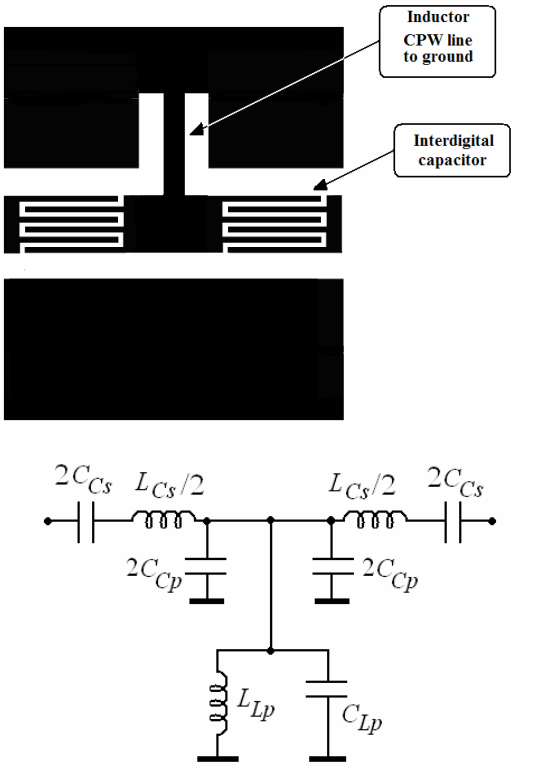

Fig. 1. Layout of a CRLH structure (a) and its equivalent circuit (b).

It is possible to show that the frequency band of a balanced CRLH structure, $f_{max} - f_{min}$, is given by the following cutoff frequencies at 3 dB:

$$f_{min} = \frac{f_{c_{LH}}}{2}\left[\sqrt{1+\frac{4f_{c_{LH}}}{f_{c_{RH}}}}-1\right] \quad (1a)$$

$$f_{max} = \frac{f_{c_{RH}}}{2}\left[\sqrt{1+\frac{4f_{c_{LH}}}{f_{c_{RH}}}}+1\right] \quad (1b)$$

where:

$$f_{c_{LH}} = \frac{1}{4\pi\sqrt{L_{Lp}C_{Cs}}} \quad (2a)$$

is the cutoff frequency of the LH (Left-Hand) mode and

$$f_{c_{RH}} = \frac{1}{\pi\sqrt{L_{Cs}C_{Cp}}} \quad (2b)$$

is the cutoff frequency of the RH (Right-Hand) mode.

Using modelling software IE3D-Zeland (full-wave 3D) and Microwave Office were used. The previous relations one may find that for $f_{min} \cong 20$ GHz and

$f_{max} \cong 75$ GHz one obtain 30 GHz and $f_0 = 40$ GHz where $f_0 = k \times f_{c_{LH}} = k / f_{c_{RH}}$ and k is a dimensionless design parameter, k > 1; here k = 1.3. The design of CRLH structure was performed for a characteristic impedance $Z_c = 50\ \Omega$.

2.2. Design of interdigital capacitor

The layout of interdigital capacitor is shown in figure 2a. The geometrical dimensions of this capacitor were calculated in order to obtain the desired values for C_{Cs} and for the series resonance frequency f_0. So, for $f_0 = 40$ GHz and $Z_c = 50\ \Omega$ results a value $2C_{Cs} \cong 106$ fF.

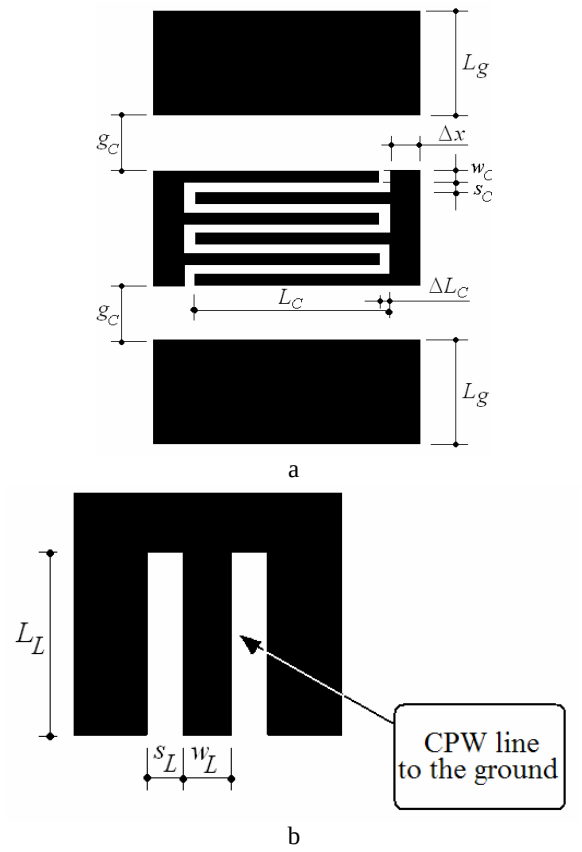

Fig. 2. (a) The schematics of the interdigital capacitors in CPW tehnics. (b) Layout of the CPW inductive stub. The structures dimensions are w_C = 10 μm, s_C = 5 μm, L_C = 250 μm, ΔL_C = 5 μm, Δx = 20 μm, g_C = 65 μm, L_C = 625 μm.

The digits length of the interdigital capacitor must be much smaller than the wavelength for f_0. So, considering the design restrictions, a value $L_c << 3000$ μm was chosen.

The value of 106 fF necessary for interdigital capacitor and the resonance frequency of 40 GHz may be obtained using the following layout dimensions shown in the figure 2a. The number of digits is n = 10 and the substrate is a high silicon wafer covered with silicon dioxide. In such conditions the values $L_{Cs} \cong 0{,}3$ nH and $C_{Cp} \cong 25$ fF are obtained (see figure 1).

2.3. Design of inductive CPW ground shorted stub

For the frequency $f_0 = 40$ GHz, the characteristic impedance $Z_c = 50\ \Omega$ and $k \cong 1{,}3$ found in the previous sub-chapter one may compute the following elements: $L_{Lp} \cong 0{,}13$ nH and $C_p = \frac{1}{\pi f_{c_{RH}} Z_c} \cong 120$ fF. Then, knowing $C_{Cp} \cong 25$fF, $C_{Lp} = C_p - 4C_{Cp} \cong 20$ fF results.

The resonance frequency of the inductor will be: $f_{0_L} = \frac{1}{2\pi\sqrt{L_{Lp} C_{Lp}}} \cong 97$ GHz.

The inductive ground shorted CPW stub was designed to obtain the above presented values: $L_{Lp} \cong 0{,}13$ nH, $C_{Lp} \cong 20$ fF ($f_{0_L} \cong 97$ GHz.) and $Z_{cl} \cong 62\ \Omega$. The layout physical dimensions: $L_L = 277$ μm, $w_L = 42$ μm and $s_L = 10$ μm are indicated in Fig. 2b.

With this, all the elements of the equivalent circuit in figure 1b are known. The CRLH cell shown in figure 1a was analysed with Microwave Office software and the results are presented in figure 3. The scattering parameters S_{11} and S_{21} characterise the microwave transmission line and are the equivalent of reflectivity and transmissivity coefficients.

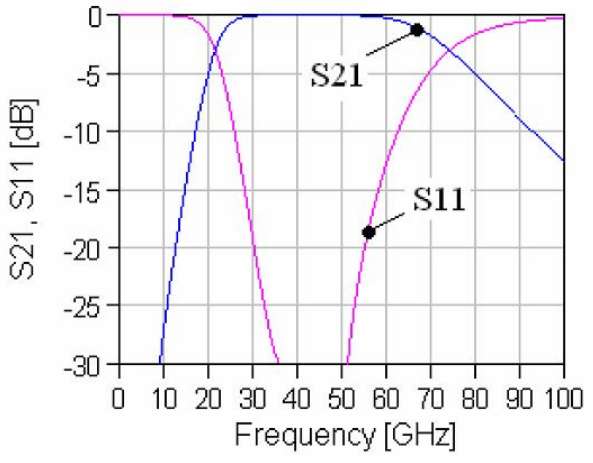

Fig. 3. Scattering parameters S_{11} and S_{21} calculated from the equivalent circuit of the CRLH structure.

One may observe that f_{min} and f_{max} are practically the same as the imposed values (20 GHz and 75 GHz, respectively), and the reflexion losses are small, proving that the circuit elements were correctly designed.

3. Fabrication of CRLH structures

3.1. The experimental setup

The equipment used to create the periodic microstructures is a standard laser microprocessing setup, coupled with a commercial laser system Clark CPA-2101, delivering ultrafast pulses of 200 fs duration, 775 nm wavelength, and 2 kHz repetition rate. The measured laser beam quality factor M^2 is 1.5 and the beam diameter is 4 mm. The laser pulses are attenuated in the range of tens to hundreds of nJ. The laser beam is focused by a 20x microscope objective with 0.4 numerical aperture and 7 mm entrance aperture. The beam waist was w_0 = 3.1 μm. The samples are precisely translated and positioned by a XYZ fine translation stage, equipped with stepper motors which provide travel range of 50 x 50 x 25 mm^3, and precision displacement of the order of hundreds of nm. The optimum scanning speed was established to be 0.2mm/s for minimising mechanical positioning errors and for a reasonable processing time. Thus, we can estimate the spacing between two sequent pulses to be 0.1 μm. Since the focused spot diameter is 6.2 μm, we obtain a multipulses ablation regime with about 62 pulses per shot. The focalization is controlled by an optical visualization system with CCD, with overall optical resolution of 1 μm.

3.2. Control parameters of the laser ablation

For the fabrication of the CRLH structure with the designed geometry we are limited by some constraints. First of all, the width of the ablated grooves has to be well controlled with submicrometer precision, and secondly, the substrate has to be not affected by the laser processing. Then, we perform preliminarily studies of the ablation parameters of the gold film in order to establish the optimal ablation parameters. The minimum laser fluence required to completely and uniformly ablate the 100 nm thick gold film and the 20 nm of Cr layer was measured as F_{th}= 1.2 J/cm^2 in our experimental configuration. This value is much higher compared to the ablation threshold of 0.14 J/cm^2 reported by other works [17-18]. However, if laser processing takes place just above the ablation thresholds, the ablation depth is at the order of few tens on nm, not enough to completely remove the metallic film. The presence of the 20 nm of Cr layer will also require a slightly increase of the laser fluence compared with the case of a simple gold film. Since the Cr film is much thinner compared with the Au film, and the ablation threshold of Cr is lower compared with the gold films, the Cr is completely ablated simultaneously with the Au film, for the high enough laser fluence. The ablation selectivity between metals and the SiO_2 isolator layer is assured by the much higher ablation threshold of the latter one. For lower laser fluences and/or lower number of pulses, the Au and the Cr films are incompletely or non uniformly ablated producing CRLH structure with short-circuited capacitors.

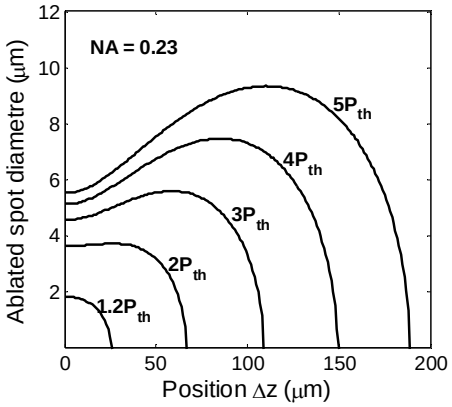

a

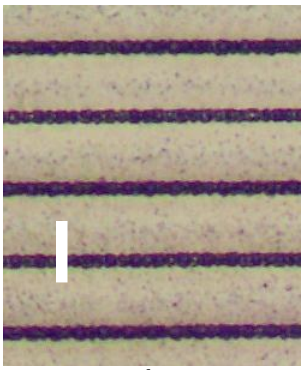

b

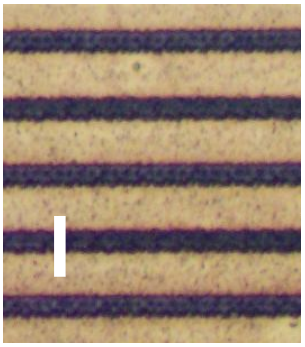

c

Fig. 4. (a) The diagrams of the ablated spot size as a function of the focus position z for different laser intensities larger than the ablation threshold. The grooves created on gold film by laser ablation have: (b) 2.5 μm width for unfocused configuration at z = 80 μm, and (c) 5μm width at Δz = 40 μm. The laser energy was 200 nJ/pulse. Scale bar is 15 μm.

The ablated volume is given by the laser irradiance distribution in near-field. The ablation can be controlled by the incident laser intensity, the numerical aperture *NA*

of the microscope objective, and the focus position. In the figure 4 is presented a diagram of the theoretical estimation of the ablation spot diameter in function of the focus position at different laser power levels larger that the ablation threshold. For an accurate estimation of this diagram, the effective numerical aperture NA_{eff} of the microscope objective has to be considered taking into account the incident beam diameter D = 4 mm at the input of the focusing lens. In our setup the microscope objective has a defined NA = 0.4, for an input aperture D' = 7 mm. In this case, the effective numerical aperture becomes $NA_{eff} = D/D' NA = 0.23$. For this value the focused beam has a beam waist w_0 = 3.1 μm and the confocal parameter z_R = 38 μm.

The radial intensity distribution of the gaussian beam at a given z position is described by the relation:

$$I(r,z) = \frac{2P}{\pi w(z)^2} \exp\left(-\frac{2r^2}{w(z)^2}\right), \qquad (3)$$

where $w(z)$ is the beam radius at z position from the focus plane.

If the laser power P_{th} is the smallest power for which we obtain an uniform and complete ablation of the film in well focused conditions for a given lens, the corresponding laser irradiance in the centre of the focused spot is $I_{th} = \frac{2P_{th}}{\pi w_0^2}$. For any other power of the incident laser and any focalisation position of the lens, the boundary of the ablated area can be defined as the r position where the laser irradiance $I(r,z)$ has the threshold value I_{th} . With this assumption, knowing experimentally the ablation threshold, we will estimate the diameter of the ablated circular spot for any focusing position and laser intensity as in the diagrams from the figure 4a.

Experimentally we measured the width of the ablated structures on the gold film obtained by scanning the sample at different laser energies and focalisation conditions. In the figures 4 b) and c) are presented the optical microscope images for two different focusing conditions. The width of the ablated grooves is 2.5 μm when the sample is defocused with z = 80 μm from the focus plane, respectively 5 μm for z = 40 μm, at the same incident laser energy 200 nJ/pulse. Considering the diameters of the laser spot 14 μm and 9 μm at these two z positions, the laser fluence in these two cases was 1.3 J/cm^2, respectively 3.2 J/cm^2. The scanning speed was 0.2 mm/s. Therefore, increasing the laser intensity above the threshold power we can control the ablated spot size in the range of few microns by modifying the sample position in z direction.

3.3. Fabrication of the CRLH structures by controlled laser ablation

In order to prevent the sample contamination with residual material from the ablation process, the grooves larger than 10 μm on large area were obtained by classical photolithography. A periodic structure with 4 cells and total size of 4.1 mm is produced. The unit cell of the structure is 872 μm. After this first step, the details below 10 μm are obtained by laser ablation. A network of interdigital capacitors and inductances are created on gold thin film by focusing the femtosecond laser at controlled z position in order to obtain the desired groove's width. The design is obtained by PC controlled displacement of the sample with submicrometer precision.

In the figure 5 is presented the produced CRLH device using the following parameters: laser fluence F = 3.2 J/cm^2, spot beam diameter 9 μm at z = 40 μm from the focus plane and the scanning speed 0.2 mm/s. The obtained digits width is s_C = 10 μm, and the interdigits space is w_L = 5 μm. Hence, the ablated geometry is in good agreement with the design.

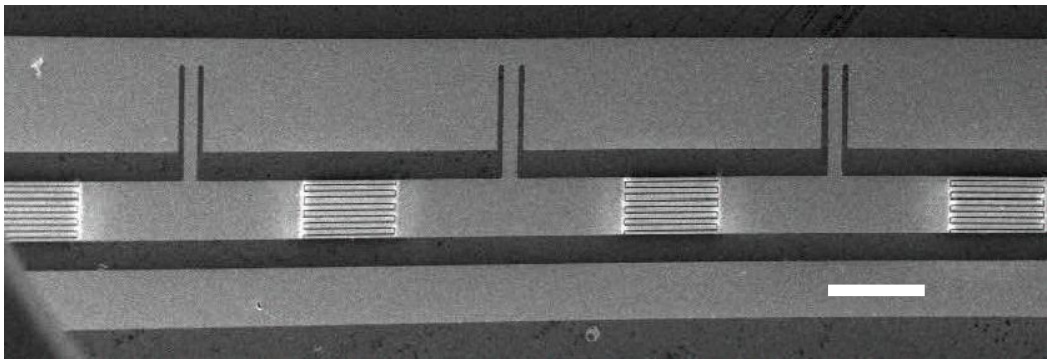

Fig. 5. The CRLH structure produced by combination of the photolithography and the ablation techniques. Scale bar: 250 μm.

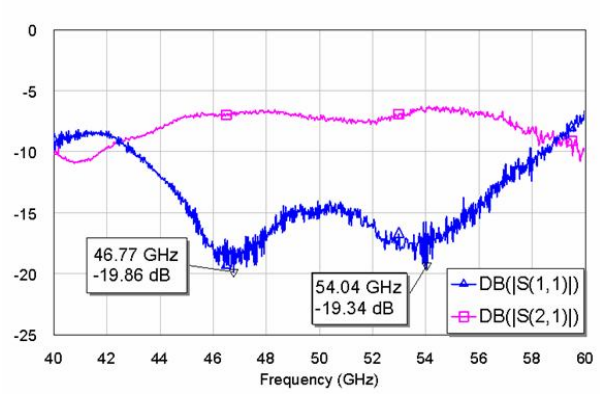

Fig. 6. The measured scattering parameters for the laser produced CRLH structure.

The scattering parameters were measured by a Karl Suss installation in combination with a Vector Network Analyzer (VNA) working in the millimetres waves range, up to 110 GHz. In the Fig. 6 the S_{11} and S_{21} parameters for the laser processed structure are presented. The central frequency of the obtained band is at 50 GHz, with a passband from 45 GHz to 56 GHz. The S_{11} parameter for this band is better than –15 dB, and S_{21} is about –7 dB for the same frequencies. The difference between the resulting CRLH structure and the designed structure could be caused by increased losses induced by contamination of the SiO_2 layer, between the capacitor electrodes, with metal nanoparticles which remain even after ultrasonic bath.

4. Conclusions

Laser ablation technique can be successfully used for configuration of micro-devices on metallic films which are difficult to be processed by traditional photolithography technique. Using the actual setup, the structures dimensions can be controlled in the range of 1 to 10 µm with resolutions below 1µm. Metamaterial based millimeter wave devices were fabricated on metallic films by laser ablation. From the calculated scattering parameter, the CRLH transmission line shows a large passband from 20 to 75 GHz. The measured scattering parameters showed similar behaviours with a slightly different passband due to the losses induced by contamination of the film during laser processing.

Acknowledgements

This work was financially supported by the National Scientific Research Agency, Project No. PN2_11-010.

References

[1] Malcolm Gower, Proc. SPIE **6879**, 687902 (2008).
[2] Satoshi Kawata, Hong-Bo Sun, Tomokazu Tanaka, Kenji Takada, Nature **412**, 697 (2001).
[3] Shigeki Matsuo, Satoshi Kiyama, Yoshinori Shichijo, Takuro Tomita, Shuichi Hashimoto, Yoichiroh Hosokawa, Hiroshi Masuhara, Appl. Phys. Lett. **93**, 051107 (2008).
[4] Tao Tong, Jinggao Li, and Jon P. Longtin, ASME Conf. Proc. 2003, 53 (2003).
[5] A. Ashkin, J.M.Dziedzic, T.Yamane, Nature, **330**, 609 (1987).
[6] J.M Liu, Opt.Lett. **7**, 196 (1982).
[7] X. Liu, D. Du, G. Mourou, IEEE J. Quantum Electron, **33**, 1706 (1997).
[8] P.P. Pronko, SK. Dutta, J. Squier, J.V. Rudd, D. Du, G. Mourou, Opt. Comm. **114**, 106 (1995).
[9] Julia Eizenkop, Ivan Avrutsky, Gregory Auner, Daniel G. Georgiev, and Vipin Chaudhary, J. Appl. Phys, **101**, 094301 (2007).
[10] Z. B. Wang , B.S. Luk'yanchuk, L. Li, P.L. Crouse, Z. Liu, G. Dearden and K.G. Watkins, Appl. Phys. A: Materials Science & Processing, **89**, 363 (2007).
[11] Eric Betzig, Jay K. Trautman, Science **257**, 189 (1992).
[12] M. Ohtsu, H. Hori, Near-field Nano-optics (Kluwer Academic, NewYork, 1999).
[13] C. Caloz, T. Itoh, Electromagnetic metamaterials: transmission line theory and microwave applications, John Wiley & Sons, (New Jersey, 2006) p.128.
[14] R. Marques, F. Martin, M. Sorolla, Metamaterials with negative Parameters:Theory Design and Microwave Applications, John Wiley & Sons, 2008.
[15] G.V.Eleftheriades, K.G.Balmain, Negative-refraction Metamaterials: Fundamental Principles and Applications, John Wiley & Sons, 2008.
[16] M. Zamfirescu, R. Dabu, M. Dumitru, G. Sajin, F. Craciunoiu, Journal of Laser Micro/NanoEngineering, **3**, 5 (2008).
[17] Mikhail E. Povarnitsyn, Konstantin V. Khishchenko Pavel R. Levashov, Appl. Surf. Science, **255**, 5120 (2009).
[18] J. Hermann, S. Noel, T.E. Itina, E. Axente, M. E. Povarnitsyn, Laser Phys., **18**, 374 (2008).

*Corresponding author: marian.zamfirescu@inflpr.ro